

General Disclaimer

One or more of the Following Statements may affect this Document

- This document has been reproduced from the best copy furnished by the organizational source. It is being released in the interest of making available as much information as possible.
- This document may contain data, which exceeds the sheet parameters. It was furnished in this condition by the organizational source and is the best copy available.
- This document may contain tone-on-tone or color graphs, charts and/or pictures, which have been reproduced in black and white.
- This document is paginated as submitted by the original source.
- Portions of this document are not fully legible due to the historical nature of some of the material. However, it is the best reproduction available from the original submission.

NASA

Technical Memorandum **80556**

**Magnetic Field Studies at
Jupiter by Voyager 2:
Preliminary Results**

**N. F. Ness, M. H. Acuna,
R. P. Lepping, L. F. Burlaga,
K. W. Behannon and F. M. Neubauer**

(NASA-TM-80556) MAGNETIC FIELD STUDIES AT
JUPITER BY VOYAGER 2: PRELIMINARY RESULTS
(NASA) 27 p HC A03/MF A01 CSCL 03B

N79-34138

Unclas

G3/91 38917

AUGUST 1979

National Aeronautics and
Space Administration

Goddard Space Flight Center
Greenbelt, Maryland 20771



Magnetic Field Studies at Jupiter By Voyager 2:
Preliminary Results

Submitted to Science 9 August 1979

Introduction

The Voyager 2 magnetic field experiment is identical to that on Voyager 1 (1) and operated flawlessly throughout the second Jupiter encounter. This paper presents a brief overview of the results obtained to date on the Jovian magnetosphere, the bow shock, the magnetopause, and the extended magnetic tail, which was first identified and studied in Voyager 1 data (2). Because the radius of the tail on the dawnside of the magnetosphere is so large (150-200 R_J) and the post-periapsis trajectory was at a sun-planet spacecraft angle of 140° , Voyager 2 was immersed in the tail for approximately 2 weeks. Two crossings of the near equatorial current sheet (plasma sheet) were observed in the magnetosphere and its tail almost every 10 hour rotation period of the planet. Hence, a definitive mapping of the geometry and character of these enhanced plasma and depressed magnetic field regions has been possible far into the nightside tail region. At periapsis the observed field is 335 nT (nanotesla), 20% less than the expected 425 nT, and this is due to the immersion of Voyager 2 in the current sheet.

In addition, evidence is found for an interaction of the satellite Ganymede with the Jovian magnetosphere, which leads to disturbances observed forward of this satellite as the Jovian magnetosphere co-rotates with the planet past the satellite. The character of these disturbances is complex. Their spatial location suggests that the magnetosphere may be in motion with respect to the planet at the satellite distance of 15 R_J .

The data presented utilize averages of the basic vector field measurements (at 16 2/3 Hz) over intervals of 1.92 seconds, 9.6 seconds, 16 minutes and 1 hour. As in the 30 day report on Voyager 1 results, these data and interpretations are preliminary and based on quick look data tapes and ephemerides.

Bow Shock and Magnetopause

Voyager 2 crossed the bow shock of Jupiter inbound at least eleven times from day 183 (2 July) 1979 at 1621 universal time (UT) to day 186, 0955 UT. This corresponds to a planetocentric distance range of 98.9 to 66.5 R_J (R_J = radius of Jupiter). Fig. 1 shows the trajectories of Voyager 1 and 2, as well as Voyager 1's modeled bow shock and magnetopause boundaries (1). The first and last inbound bow shock encounters (filled circles) are shown for Voyager 2, and a representative set of Voyager 1 inbound bow shock crossings are given. Voyager 2 crossed the magnetopause three times inbound to Jupiter, the first occurring on day 185 at 2337 UT and the last on day 186 at 1840 UT, also shown in Fig. 1. The upper two panels of Fig. 2 (B and RMS vs. time) show identifications of the inbound magnetopause and bow shock crossings.

In order to obtain an estimate of the average bow shock normal direction over seven of the eleven crossings, magnetic coplanarity was used where applicable, and linear field component averaging was applied for "parallel" shocks (i.e. those for which the shock surface normal is parallel to the upstream magnetic field). Preliminary results in heliographic coordinates were:

$$\langle \lambda \rangle = 180^\circ \pm 19^\circ \quad \text{and} \quad \langle \delta \rangle = 30^\circ \pm 38^\circ,$$

where λ and δ are, respectively, the longitude and latitude referenced to the solar equatorial plane ($\lambda = 180^\circ$ is sunward and $\delta = 90^\circ$ is "northward"). Due to the large variability of the data around most of the bow shock crossings, reflected in part by the large uncertainties on $\langle \lambda \rangle$ and $\langle \delta \rangle$, a meaningful comparison with the modeled hyperbolic bow shock normal ($\lambda_{\text{model}} = 160^\circ$, $\delta = 0^\circ$) based on the Voyager 1 crossings is impossible. The second and third magnetopause crossings were analyzed by determining for each the plane of minimum variance (3) of the magnetic field through the transition zone using 1.92-second averages. The analyses yielded $\lambda_2 = 156^\circ$, $\delta_2 = -3^\circ$ for the second crossing and $\lambda_3 = 154^\circ$, $\delta_3 = 1^\circ$ for the third. The magnetopause crossings were classic tangential discontinuities.

Preliminary analysis of the first magnetopause crossing, which was unusually broad and turbulent, has not yielded meaningful results.

As of this date (2 August 1979) no outbound bow shock crossings have yet been identified. Although no unambiguous outbound magnetopause crossings have been distinguished, the magnetic field data on days 204 - 206 show characteristics of the magnetosheath. However, periods of tail-like data were also observed during these and many following days. As shown in Fig. 2, an obvious change in the character of the field, on this time scale, had taken place during days 204 - 206. Before this period, starting at about the beginning of day 193 ($35 R_J$) the field appeared in all respects like a magnetospheric tail; this region will be discussed below. The data gap from day 204, 1616 UT to day 205, 0036 UT is due to permanent data loss during a spacecraft trajectory course maneuver.

Since no clear Voyager 2 outbound magnetopause crossing has yet been identified, an accurate estimate of an average modeled magnetopause surface is impossible to derive at this time. However, since the magnetopause as observed by Voyager 1 was successfully modeled by an X-axis symmetric parabola in Jupiter's orbital plane, a similar geometry was used to predict the region where Voyager 2 outbound might be expected to encounter the magnetopause. This curve depends only on the average position of the Voyager 2 inbound magnetopause crossings and the average normal to that surface at that point. From the results of analyzing multiple intervals associated with the second and third crossings, this normal is $\langle \lambda \rangle = 152^\circ$, $\langle \delta \rangle = 0^\circ$. This information is sufficient to produce the modeled Voyager 2 magnetopause (MP-V2) shown in Fig. 1, which is analytically represented by $Y = \pm 10.1(68.2 - X)^{1/2}$, where X and Y are in units of R_J . This curve intersects the outbound trajectory on mid-day 208, and yields a solar wind stagnation point of $68 R_J$. The uncertainty in the estimated average inbound bow shock normal is obviously too large to carry out a similar procedure for the bow shock.

Magnetosphere Structure

From Fig. 2, it is clear that a principal feature of the magnetic field observations throughout the encounter is the persistent 10 hour periodicity in the occurrence of two dips in the field magnitude each accompanied by an increase in the Pythagorean mean RMS. These events correspond to traversals of the near equatorial current sheet of the inner magnetosphere or to traversals or close approaches to the plasma sheet in the magnetic tail. They are quite similar to the events shown in Fig. 4 of the Voyager 1 paper (1).

Inbound and near Jupiter the magnetic field vector is always directed southward, consistent with the polarity of the main planetary field. In the tail, beyond $50 R_J$, the vector tends to be parallel to the plasma sheet and the expected position of the magnetopause. The field depressions are often very significant, amounting to 80% or more of the ambient field on either side of the event. Multiple traversals or close approaches to the current or plasma sheet are also often seen. Away from the current (plasma) sheet, the field tends to slowly increase to a maximum at a point nearly midway between the adjacent sheet crossings and the RMS is very small. The direction of the field is nearly radial with respect to Jupiter close to the planet and outbound beyond $50 R_J$ where the characteristic tail geometry becomes dominant.

As the spacecraft left Jupiter, the character of the field changed from roughly dipolar with superimposed depressions near the sheet crossings to a tail configuration. Fig. 3 presents the 8 day interval from periapsis to $108 R_J$, illustrating the orientation of the field vector. The nearly step function nature of the two angles λ , δ testifies to the clear distinction of the field line source, i.e. northern ($\lambda \approx 0-20^\circ$) or southern ($\lambda \approx 180-200^\circ$) hemisphere. Close to Jupiter ($R < 30 R_J$), δ is always significantly negative (i.e. southward) but beyond that point δ approaches zero as the tail field configuration is developed.

The observations are uniformly described by the above remarks, with a few specific and, we believe, significant exceptions. Just after crossing the magnetopause while inbound, and continuing for approximately 30 hours thereafter, the magnetic field magnitude and direction fluctuated considerably. The field remained generally southward directed but with no evidence for a 10 hour periodicity in either magnitude or direction. The general appearance of the data and the magnitude of the field distinguishes the region clearly from the magnetosheath; it appears to be a type of boundary layer between the sheath and the co-rotating magnetosphere. Further examination of this particular period of data will benefit by comparisons with data from other instruments on Voyager 2 and also Voyager 1 and Pioneers 10 and 11 data.

The periapsis distance of Voyager 2 was $10.1 R_J$, twice that of Voyager 1 ($4.9 R_J$) and much more than those of Pioneer 10 and 11 (2.8 and $1.7 R_J$). As a result, it has not been possible to conduct an analysis of the main planetary field in the same manner used in these earlier studies, since the observations contain important and non-uniform contributions from localized sources near the spacecraft. Fig. 4 illustrates this point, where a comparison of the expected planetary field is made with the observed field magnitude. The large depressions which occur near the equator crossings almost merge into a continuously depressed field while the spacecraft was within $16 R_J$ of the surface of Jupiter. We have chosen to postpone any quantitative analysis of the main field, due to the large contribution from local and external sources. The reader may recall that on Voyager 1, the preliminary report (1) showed that the dipole term was smaller by 5% than that obtained by Pioneer 11. This was interpreted to be due to the magnetic field of the current sheet; even though the maximum field for Voyager 1 was 8 times that of Voyager 2, the contributions from external sources were important. As Fig. 4 shows, the perturbations in magnitude amount to as much as 30% of the background field, so that the energy density of the field itself has been reduced by one-half.

Tail Structure and Dynamics

As with Voyager 1, the current sheet in the near-planet tail was found to be a broad feature with relatively shallow depressions in field magnitude. In these respects it more closely resembles the dayside current sheet than that of the more distant tail. There the sheet crossing signature in the magnetic field is generally a very rapid direction change together with a deep depression in the field magnitude to near zero. In Fig. 5 the spacecraft locations at the times of magnetotail sheet crossings are shown. Fig. 5a also includes curves giving the sheet crossing longitudes as functions of radial distance according to various theoretical models: the rigid magnetodisk (5) and two non-rigid models (6,7).

The observed crossings agree with the rigid model near the planet, as previously observed (1), and then gradually exhibit an increasing delay with increasing radial distance. An asymmetry is found between the two types of crossings, however. The north-to-south tend to follow the K model (6) curve, but the return crossings do not. The south-to-north sheet crossings most nearly agree with the N model (7), but that model does not fit the north-to-south crossings. A lack of symmetry was also observed by Voyager 1, where the south-to-north longitudes were not too different from those expected for the rigid model, whereas the north-to-south crossings were closer to the curve for a disk with spiral distortion.

In Fig. 5b the current sheet crossings are shown in terms of the solar magnetospheric coordinate Z_{SM} . The solar magnetospheric (SM) coordinates form a right-handed, non-rotating, orthogonal system defined such that X_{SM} is directed from the planet to the sun and Z_{SM} lies in the plane containing the X_{SM} axis and M , the magnetic dipole moment of the planetary field. Voyager 1 found that within a radial distance of $25 R_J$, the current sheet crossings occurred nearly coincident with the spacecraft traversal of the magnetic equatorial plane, while in the outer portion of the outbound traversal of the pre-dawn magnetosphere, the sheet crossings occurred generally near or

south of the SM equatorial plane (2). Voyager 2 data support this view in which at increasing planetocentric distances there is a transition from an equatorial current sheet to a tail current sheet which is approximately parallel to the SM XY-plane, although somewhat south of it, as seen in Fig. 5b. Figs. 5a and b both illustrate the temporal variability of the Jovian magnetotail structure. On four occasions at $R < 140 R_J$ complete crossings of the current sheet were not observed, although perturbations of the magnetic field were seen.

Fig. 6 shows hourly average tail field vector components projected on the SM equatorial plane. The length of the field vectors was scaled logarithmically as $K (1 + \log B_{XY})$, with representative values of 1 and 100 nT illustrated. The periodic traversal of the current sheet behind the dawn-dusk meridian to a distance of $\sim 96 R_J$ is evident in the alternating direction of the vectors in this projection. There may also have been additional traversals at greater distances. Other than the data near the end of the trajectory segment shown, the few vectors in Fig. 6 which do not have the characteristic magnetotail orientation represent hours dominated by current sheet crossings, with changing azimuthal direction and a large, generally southward Z component. North (south) of the current sheet the field was directed parallel (antiparallel) to $\lambda \sim 18^\circ$ in the near-planet portion of the tail, veering gradually to $\lambda \sim 12^\circ$ or less at greater distances.

In summary, Voyager 2 has confirmed that current sheet crossings in the more distant ($X_{SM} < -25R_J$) magnetotail are not symmetrical with respect to occurrence longitude in contrast to predictions by the various existing theories. The crossings are reasonably well understood in terms of a periodic rocking of the tail current sheet about the longitudinal axis of the tail, as Jupiter rotates, in a fashion similar to that observed in Earth's magnetotail. Temporal variations are sometimes seen which perturb the normally steady magnitude and direction of the tail field and alter the location as well as other characteristics of the current sheet for periods of hours. Whether these disturbances are due to external (solar wind)

variations or to internal dynamical processes is not yet known but may be clarified through careful correlation of simultaneous observations (with appropriate time delay) by Voyager 1 and 2.

Disturbances near Ganymede

Voyager 2 flew by Ganymede at a distance of 62,000 km from the satellite center, as shown in Fig. 7. We will consider the interaction between Ganymede and the Jovian magnetosphere to be expected on the basis of MHD theory, assuming that Ganymede, like our moon, has no magnetic field, no atmosphere, and very low electrical conductivity of its upper layers. Using an electron density of 1.5 cm^{-3} , the theoretical corotational speed of 177 km/s, a magnetic field magnitude of 120 nT and a heavy ion mix typical of Voyager-1 torus observations, we obtain an Alfvén Mach number of $M_A = 0.26$, i.e., $M_A^2 \ll 1$. Breakdown of corotation (8) and an appreciable contribution of protons would strengthen this conclusion. Assuming further that $M_S^2 \gg M_A^2$, where M_S is the sonic Mach number, we expect that there will be no bow shock, since $M_A < 1$.

Flux-tubes moving with their initial flow speed will be emptied of some of their plasma while passing Ganymede, but they will not be deflected appreciably. The void will generate a rarefaction wave with plasma filling in from above and below. As the flux-tube moves, rarefaction wave fronts propagate in both directions along B at the sound speed. The rarefaction region will not extend perpendicular to B , because of the dominance of magnetic field pressure. Thus it has the shape of a "delta-wing" of thickness $2R_{J3}$ (where R_{J3} is the radius of Ganymede) and an opening angle of $2\theta_S = 2 \tan^{-1} (M_S^{-1})$. The resulting pressure imbalance will cause a slight inward bending of field lines towards the rarefaction region leading to a small, broad depression in B outside the wing and a small increase in B inside. The bending produces Alfvén waves in a "delta-wing" shaped region with an opening angle $2\theta_A = 2 \tan^{-1} (M_A^{-1})$, which is larger than $2\theta_S$. We expect the Alfvénic perturbations to be concentrated towards the front edge of the wing. Deviations from this simple MHD picture are expected due to finite gyro-radius effects, (especially at the boundary of the rarefaction region), and due to non-stationary processes. Last but not least, an internal magnetic field (9), a tenuous atmosphere consistent with Voyager 1 UV observations (10) or

higher electrical conductivities would change this picture.

Let us now consider the magnetic field observations made near Ganymede. Unusual fluctuations in the 9.6 sec averages of the magnitude of B and large RMS variations over 9.6 sec average intervals were observed between \approx 0350 and 1200 UT on day 190 (July 9). The position of the spacecraft during this interval is indicated by the dashed lines in Fig. 7. The disturbed region extended from approximately 61 to $-56R_{J3}$ along Y, 12.5 to $39R_{J3}$ along X, and -9 to $-27R_{J3}$ along Z. The nature of the disturbances in the magnetic field intensity is illustrated in Fig. 8. The following characteristics of the disturbances are particularly significant: 1) the size of a perturbation, ΔB , is $\lesssim 5\gamma$ in a background field of 60γ to 160γ ; 2) the duration is typically of the order of a minute; 3) an exceptionally large negative perturbation ($\Delta B < 0$) is usually preceded or followed by a large positive perturbation; 4) large positive and negative perturbations may occur in nearly symmetrical pairs (Fig. 8a, b) in which the negative perturbations are on the outside and the positive perturbations are on the inside. Another characteristic of the disturbances in B, not illustrated in Fig. 8, is that the perturbations $\Delta B_{\parallel} = B_{\parallel} - \langle B_{\parallel} \rangle$ are primarily along $\langle B_{\parallel} \rangle$. These small longitudinal perturbations are unlike the large transverse field perturbations observed near Ganymede's L-shell at rather large distances from Ganymede by Pioneer 11 (11).

Comparing the magnetic field observations with the plasma fluxes observed by the PLS instrument (J. Belcher and H. Bridge, private communication), we found that most of the large perturbations in B occur at a boundary where the plasma flux changes abruptly. The negative perturbation is always on the higher flux side of the boundary. When pairs of perturbations are observed, as in Fig. 8a,b, there is a lower flux region between them. The magnitude and sign of the perturbations in B are similar to those which one expects to observe due to magnetization and perpendicular gradient drifts at the edge of a low- β cavity. We cannot, however, exclude the possibility that the field perturbations might also be due to other causes such as

waves generated by instabilities in a sheath.

There are at least three conceivable sources of the perturbations discussed above: Ganymede and its wake; the Jovian current sheet; and a temporal magnetospheric disturbance (e.g., a substorm). The possibility that Ganymede is the source of the perturbations is suggested by their proximity to it and by the fact that they are observed at nearly equal distances toward and away from Jupiter relative to Ganymede. They are not associated with just the orbit of Ganymede, since the fluctuations were not observed by Voyager 2 when it passed near the orbit as it was outbound from Jupiter on day 191. The Jovian current sheet was observed by Voyager 2 at ζ 0330, ζ 1000, and ζ 1315 UT on day 190 (July 9). Fluctuations observed during hour 10 might be related to the current sheet, but most of the fluctuations discussed above were observed away from the center of the current sheet. Conversely, no disturbances were seen near the current sheet at ζ 1315 UT. These results suggest that the current sheet was not the primary cause of the fluctuations observed near Ganymede. The possibility that the disturbances are due to a transient magnetospheric event cannot be excluded. However, it implies that the event began just as the spacecraft was at $Y = -56 R_{J3}$ and ended when the spacecraft was at $Y = 61 R_{J3}$, which seems unlikely. Furthermore, substorm-related perturbations in B_y are likely to be transverse to B_z due to field aligned currents (11), whereas we have observed perturbations that are nearly along B_z .

If the disturbances are to be attributed to Ganymede, then one must explain how they are generated and why they are seen at relatively large distances from Ganymede. Since the magnetic perturbations have the form that one expects to be associated with a current in a sheath surrounding a cavity, they can be produced by creating low density regions, which is what happens when the magnetosphere rotates past Ganymede as explained above. The observation of perturbations associated with low flux regions as far as $Y = \pm 60 R_{J3}$ can be explained by strong deviations from corotational plasma flow, both in magnitude and direction. We may,

for example, postulate long-wavelength Alfvén waves propagating along Jupiter's magnetic field with an amplitude of $\pm 2 R_J$. In order to explain the tens of large disturbances that were observed in an 8-hr period, one requires Alfvén waves with periods of the order of 30 minutes. For an Alfvén speed of the order of 1000 km/s, this implies wavelengths of the order of $25 R_J$. Such waves may be due to resonant oscillations in the Jovian magnetosphere at the position of Ganymede, analogous to those which are assumed to be related to Pc oscillations at Earth. The existence of Alfvén waves implies the existence of small fluctuations in the direction of \mathbf{B} with a period of the order of 30 min. The waves would have a radial component of velocity directed alternately inward and outward with a speed of the order of $|\delta B| V_A / B_0 \approx 100$ km/s. Finally, the motions produced by such waves would also tend to produce a relatively broad region in which energetic particles are swept out by Ganymede. Thus, the hypothesis that Alfvén waves might be present and cause a disturbance produced by Ganymede to extend to

$y = \pm 60 R_{J3}$ can be tested in future studies with the particle and field data. An alternate source of bulk plasma motions may be provided by interchange instabilities associated with the outward transport of plasma.

NORMAN F. NESS
MARIO H. ACUNA
RONALD P. LEPPING
LEONARD F. BURLAGA
KENNETH W. BEHANNON

Goddard Space Flight Center
Greenbelt Maryland 20771

FRITZ M. NEUBAUER

Technische Universität, Braunschweig
Federal Republic of Germany

References and Notes

1. K.W. Behannon, M.H. Acuna, L.F. Burlaga, R.P. Lepping, N.F. Ness and F.M. Neubauer, Space Sci. Revs. 21, 235 (1977); N.F. Ness, M.H. Acuna, R.P. Lepping, L.F. Burlaga, K.W. Behannon and F.M. Neubauer, Science, 204, 982 (1979).
2. N.F. Ness, M.H. Acuna, R.P. Lepping, K.W. Behannon, L.F. Burlaga and F.M. Neubauer, Nature (to appear 1979).
3. B.U.O. Sonnerup and L.J. Cahill, J. Geophys. Res., 72, 171 (1967); G.L. Siscoe, L. David, Jr., P.J. Coleman, Jr., E.J. Smith, and D.C. Jones, J. Geophys. Res., 73, 61 (1968).
4. M.H. Acuna and N.F. Ness, J. Geophys. Res., 81, 2917 (1976).
5. J.A. Van Allen, D.N. Baker, B.A. Randall, M.F. Thomson, D.D. Sentman and H.F. Flindt, Science, 188, 459 (1974); C.K. Goertz, J. Geophys. Res., 81, 3368 (1976); also see review by C.K. Goertz, Space Sci. Res., 23, 319 (1979).
6. M.G. Kivelson, P.J. Coleman, L. Froidevaux and R.L. Rosenberg, J. Geophys. Res. 83, 4823 (1978).
7. T.G. Northrop, C.K. Goertz and M.R. Thomsen, J. Geophys. Res., 79, 3579 (1974).
8. R.L. McNutt, Jr., J.W. Belcher, J.D. Sullivan, F. Bagenal and H.S. Bridge, Nature. (to appear 1979).
9. F. M. Neubauer, Geophys. Res. Lett., 5, 905, 1978.
10. A. L. Broadfoot et al., Science, 204, 979 (1979).
11. M.G. Kivelson and G.R. Winge, J. Geophys. Res., 81, 5853 (1976).
12. We thank our colleagues in the Voyager Project for discussions of these early results and the entire Voyager team for the success of this experiment. We also thank G. Sisk, E. Franzgrote and M. De Gyurky and C. Brower of JPL for their support; C. Moyer, J. Scheifele, J. Seek and E. Worley for contributions to the design, development, and testing at GSFC of the experiment instrumentation; and G. Burgess, T. Carleton, C. Cressy, P. Harrison, D. Howell, W. Mish, L. Klein, L. Moriarty, A. Silver, M. Silverstein, K. Simms, and T. Volmer of the data analysis team at GSFC. Finally, we thank Drs. J. Belcher and H. Bridge for allowing us to refer to their plasma data in regard to the Ganymede-related perturbations. The possibility that these disturbances might extend over a relatively large distance from Ganymede was noted by one of us in a discussion with J. Belcher concerning a plot of plasma data which he prepared. One of us, F.M. N., was supported financially by the German Ministry of Science and Technology.

Figure Captions

1) Voyager 1 (dashed) and Voyager 2 (solid) Jupiter encounter trajectories in planetocentric orbital coordinates (X-Y plane is the orbital plane, + X toward the sun, and + Z northward). The day of the year is labeled on the trajectories. Voyager 2 remained within $15 R_J$ of Jupiter's orbital plane over the interval shown. The modeled bow shock (hyperbola) and magnetopause (parabola) curves are based on average Voyager 1 and 2 crossings.

2) Magnetic field magnitude (B) and Pythagorean mean RMS deviatior (12 minute averaging intervals) for -8/+ 16 days around closest approach (CA) to Jupiter which occurred at 2230 UT on day 190, 9 July 1979. Inbound bow shock (BS) and magnetopause (MP) crossing times are denoted, as are plot scale changes. (R_J) refers to Voyager 2's planetocentric distance at the beginning of each even number day.

3) The direction of the magnetic field in heliographic coordinates, g (longitude) and w (latitude) (16 minute average intervals) for the period day 191 to mid-day 198; see text for definition of coordinates. Measurements made during the few times that the spacecraft was rolling have not been deleted.

4) Comparison of magnitude of the observed magnetic field (48 second averaging intervals) with that of the GSFC O_4 Jupiter planetary magnetic field model (4) for 38 hours around closest approach (CA) to Jupiter.

5a). Location in Jovicentric distance and system III longitude of current sheet crossings and perturbed field regions in the magnetotail out to a radial distance of $150 R_J$. Dashed curves indicate crossing longitudes as functions of radial distance predicted by the rigid rotating disk model (R) as well as the models of Kivelson et al. (K) and Northrop et al. (N).

5b). Location of sheet crossings in terms of the solar magnetospheric (SM) Z-coordinate (see text 1) of Voyager 2 during the magnetotail passage. In cases of multiple traversals, as shown in (a), only the final complete traversal of the series is shown for clarity. Those segments of the Z_{SM} vs. R position curve that indicate location south of the current sheet are shown, while the dashed lines indicate the full extent of the oscillations of the spacecraft location in this coordinate system.

6. Projection of hourly average magnetic field components on the solar magnetospheric XY-plane along the Voyager 2 outbound trajectory. Only the field vectors corresponding to even hours have been plotted. The transition from a generally steady and uniform orientation throughout the tail to the intermittent observation of disordered magnetosheath field near the end of the data shown is clearly seen.

7) Trajectory of Voyager 2 in the neighborhood of Ganymede (J3), showing the location of the region in which the magnetic field was disturbed. The Y-axis points toward Jupiter, the X-axis points in the corotation direction, and the Z-axis forms a right-handed satellite centered coordinate system. Distances are measured in units of Ganymede radii ($R_{J3} = 2635$ km).

8) Examples of perturbations in the 9.6 sec. averages of the magnetic field intensity, B , observed near Ganymede. ΔB is the change in intensity measured with respect to a 4-minute running average of B .

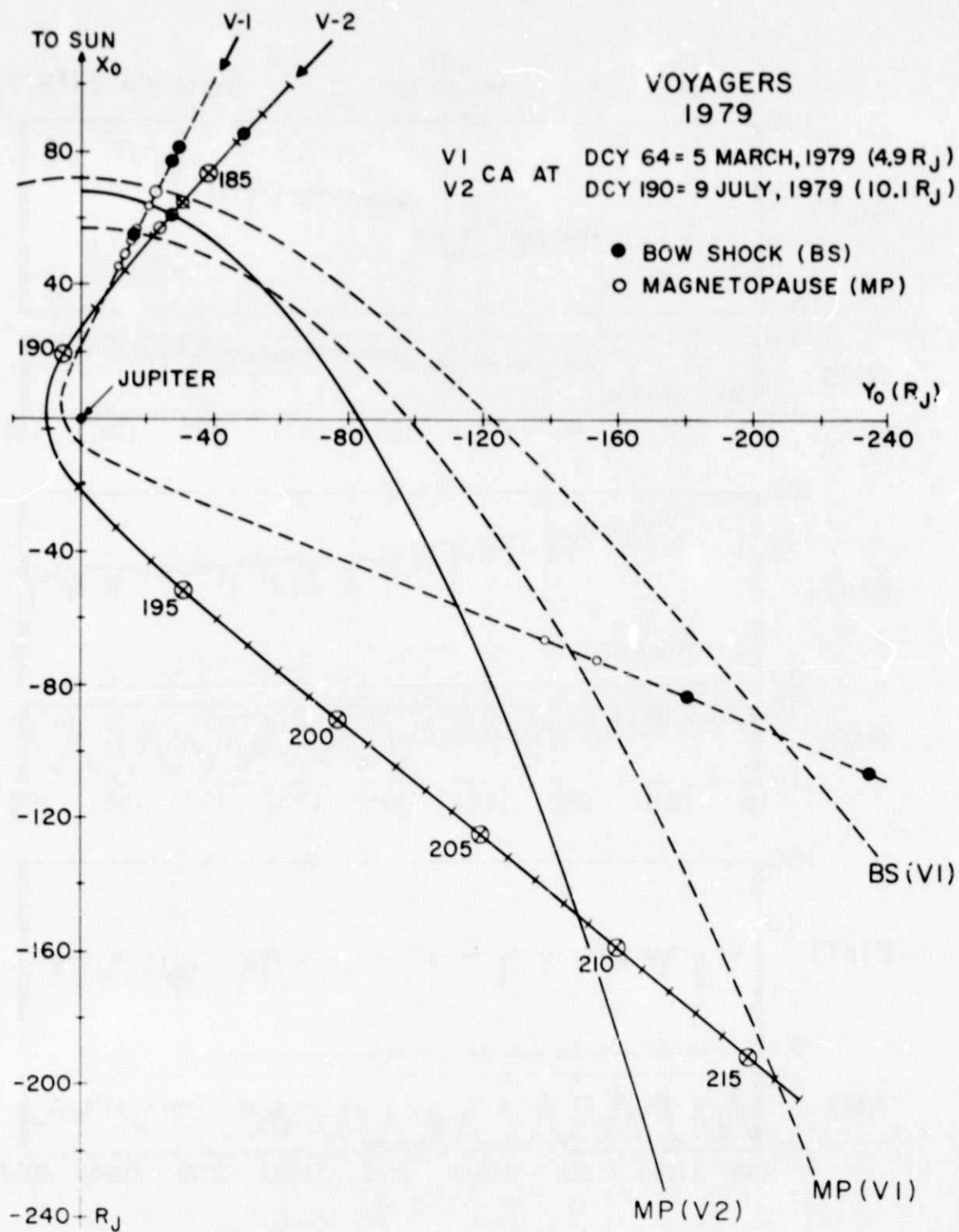


FIGURE 1

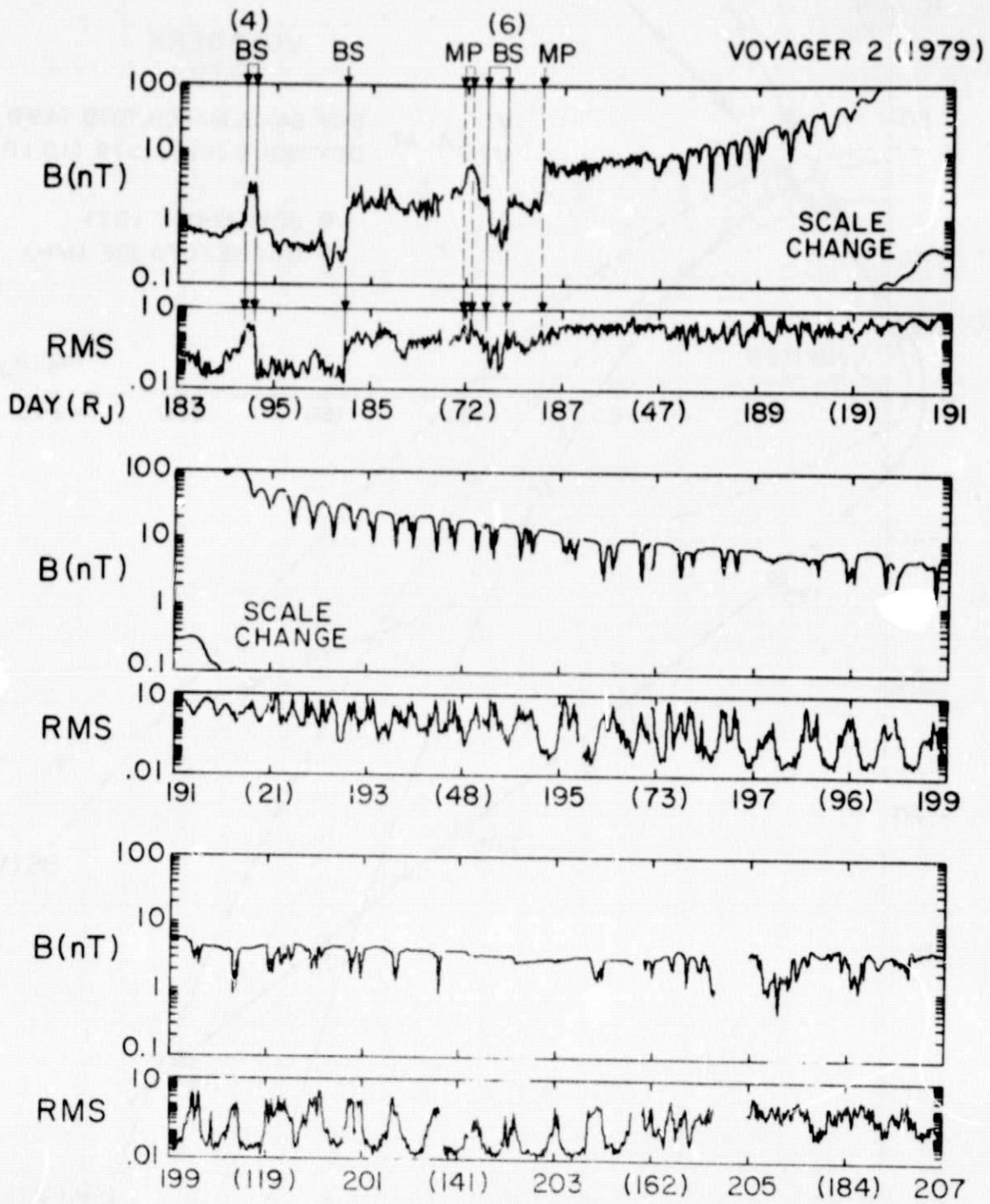
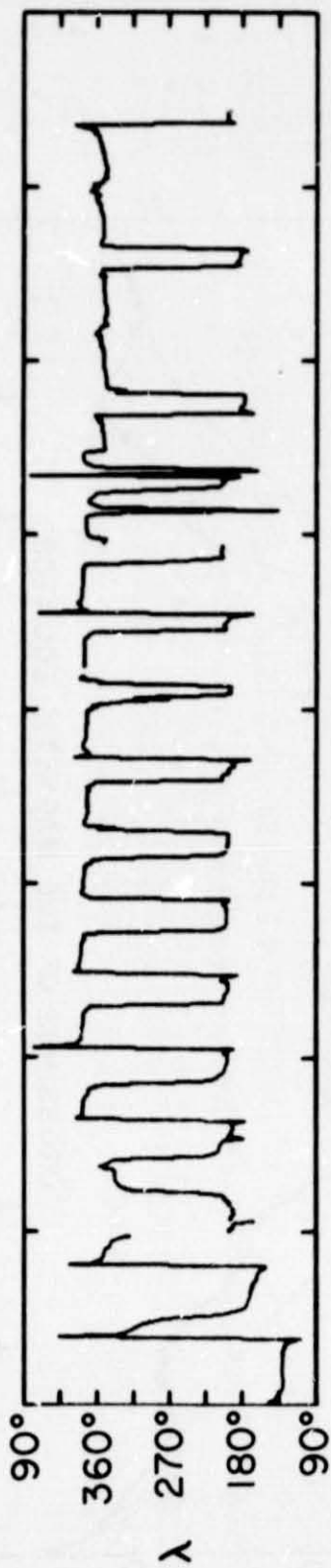


FIGURE 2

VOYAGER 2 FIELD DIRECTION



(21) (48) (73) (96)

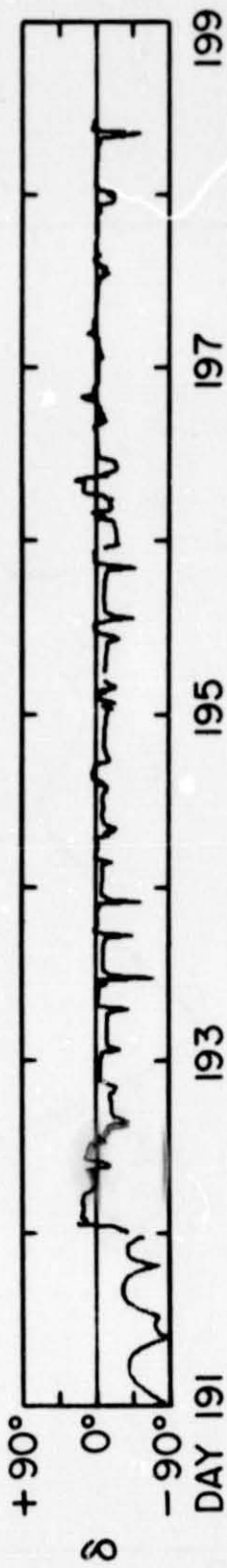


FIGURE 3

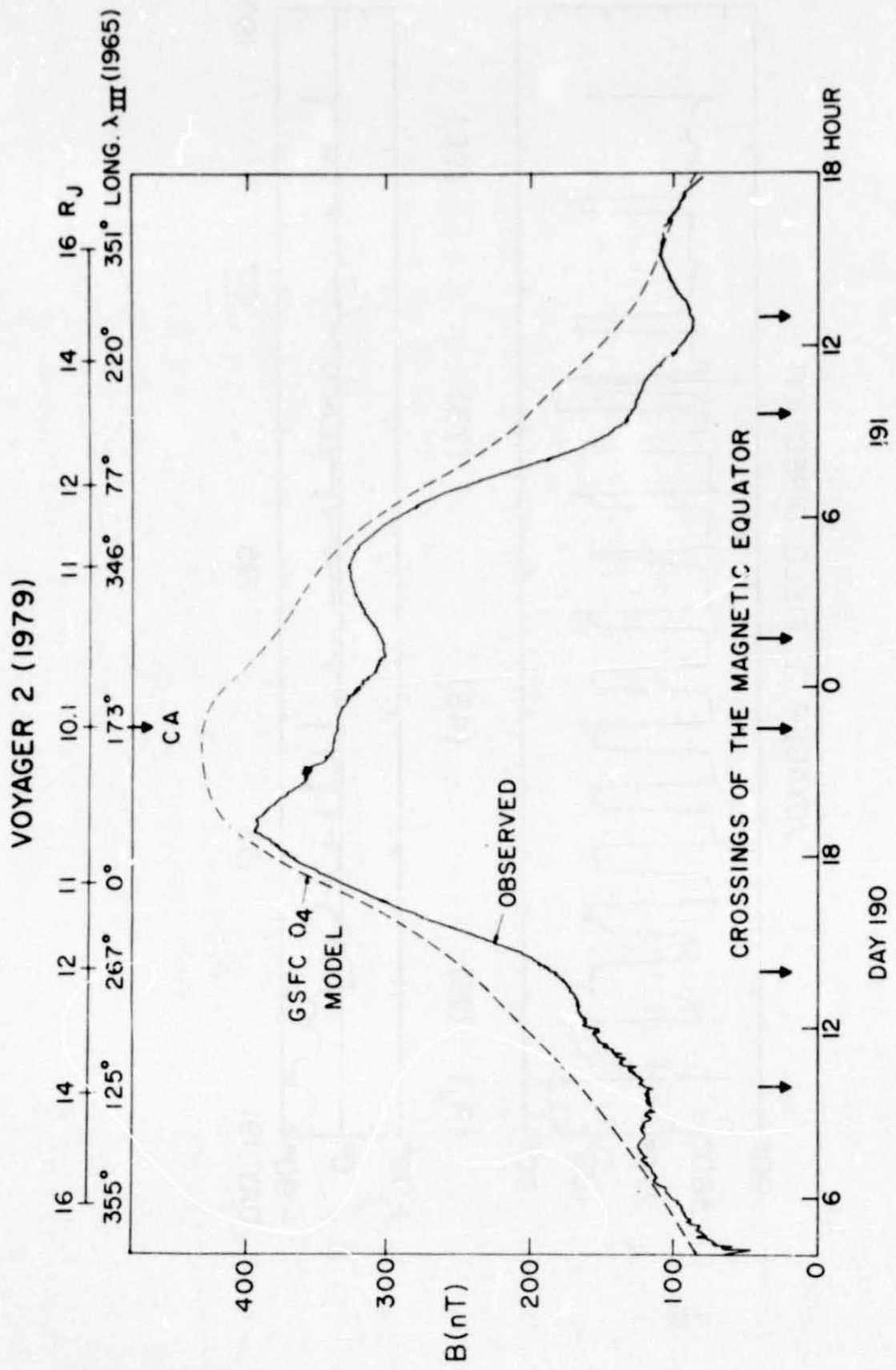


FIGURE 4

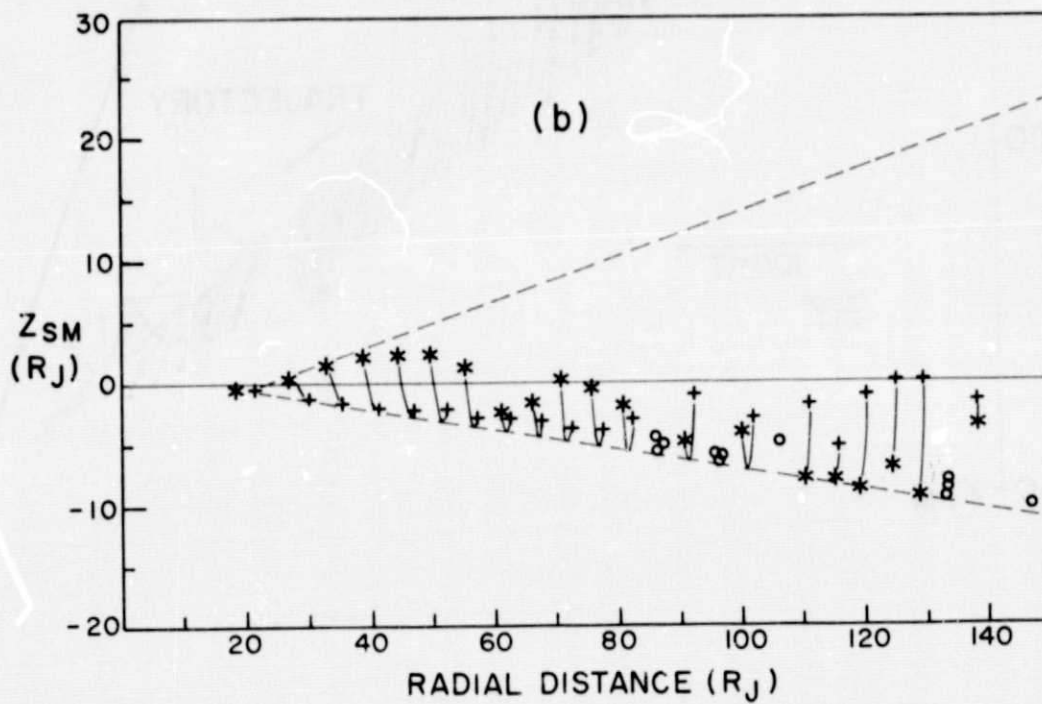
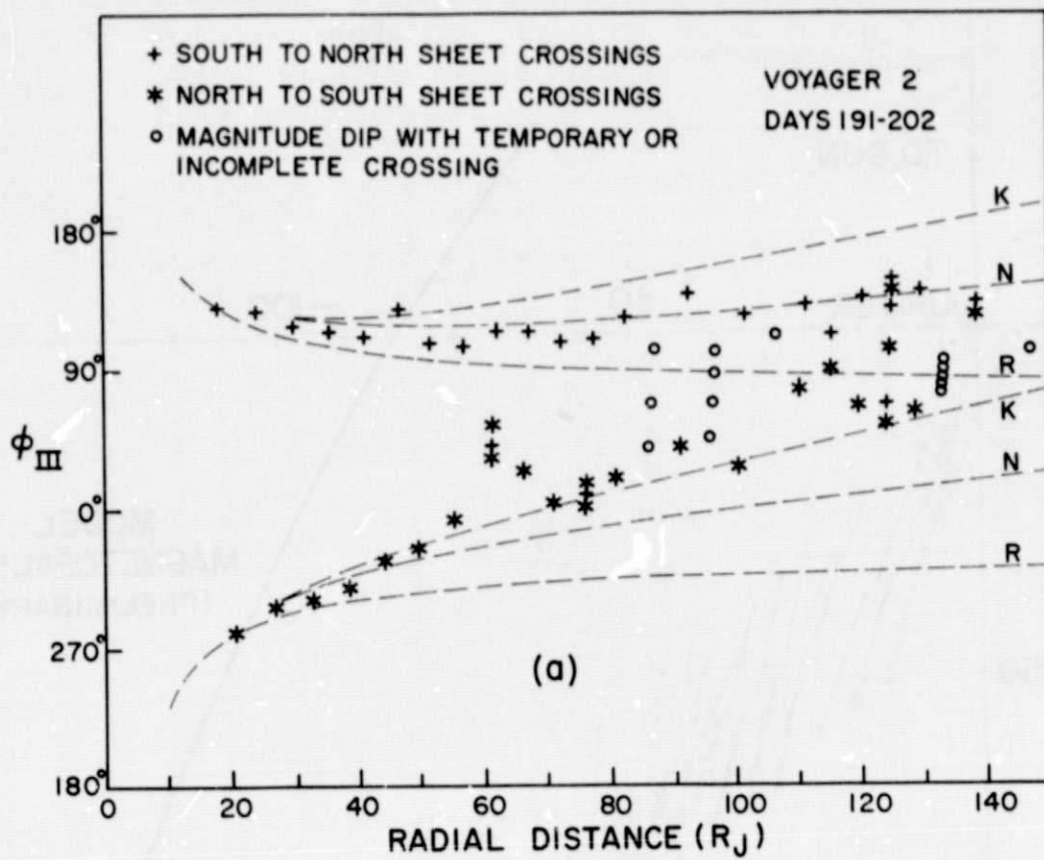


FIGURE 5

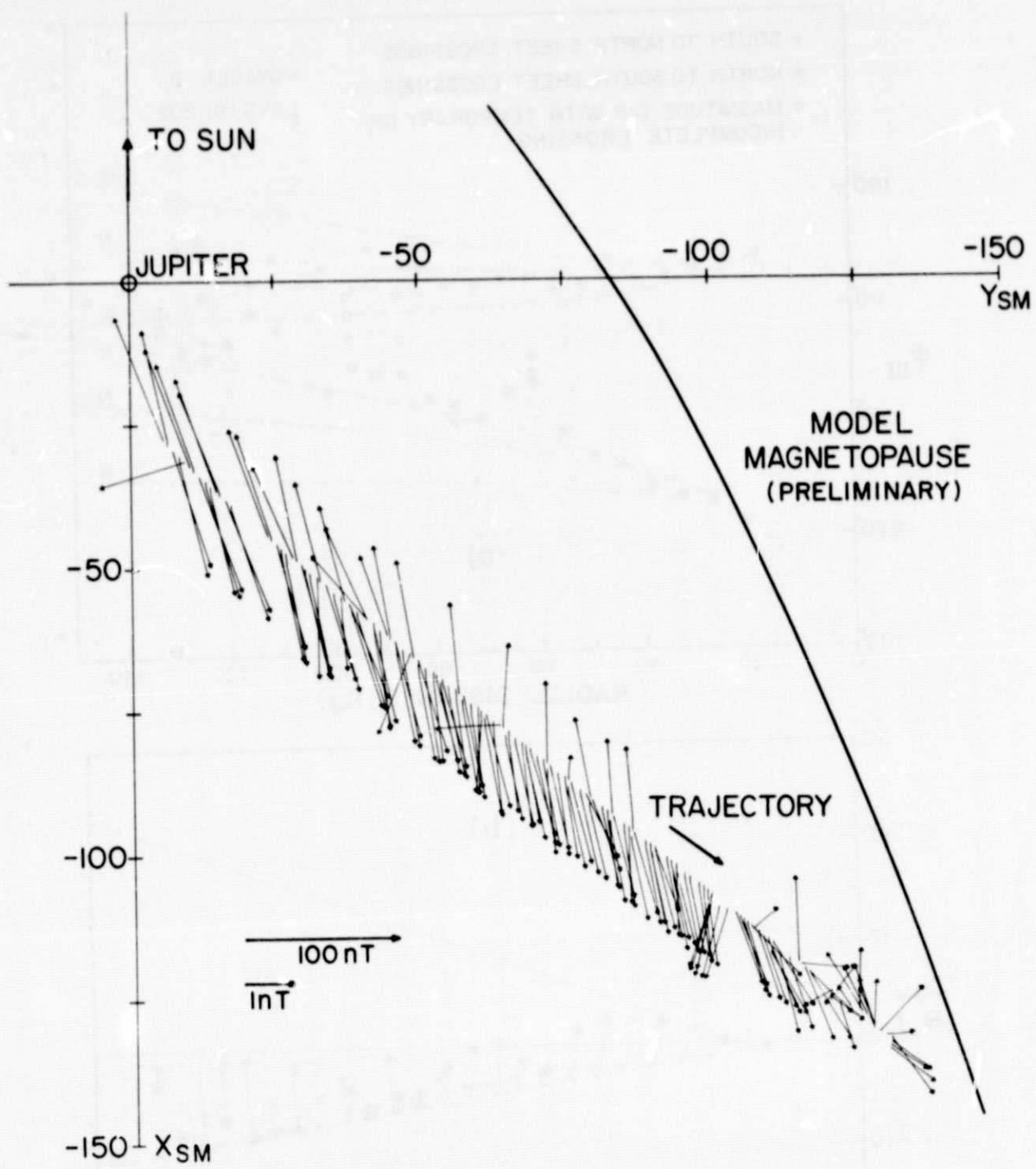


FIGURE 6

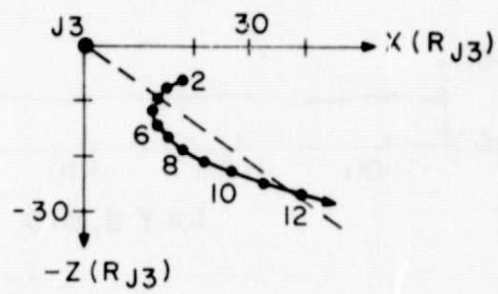
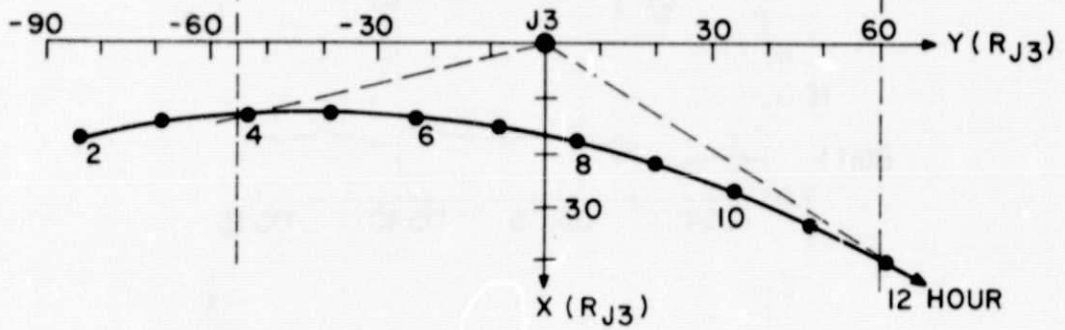
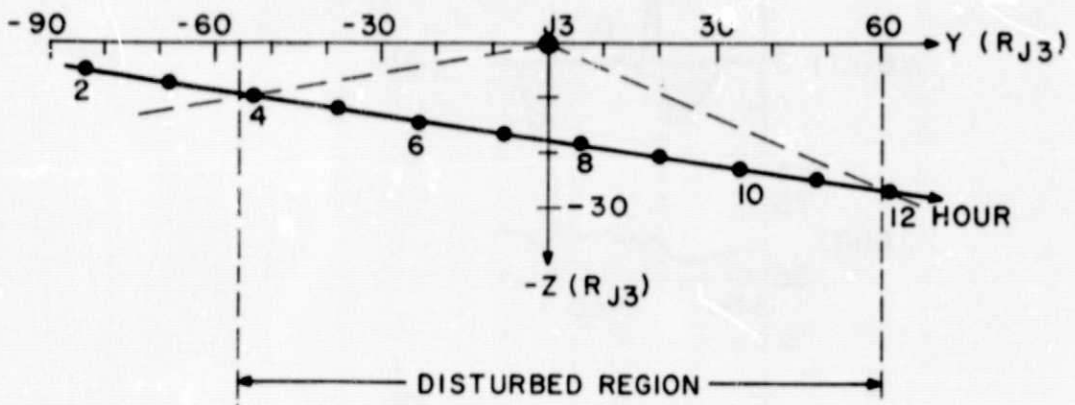


FIGURE 7

VOYAGER 2

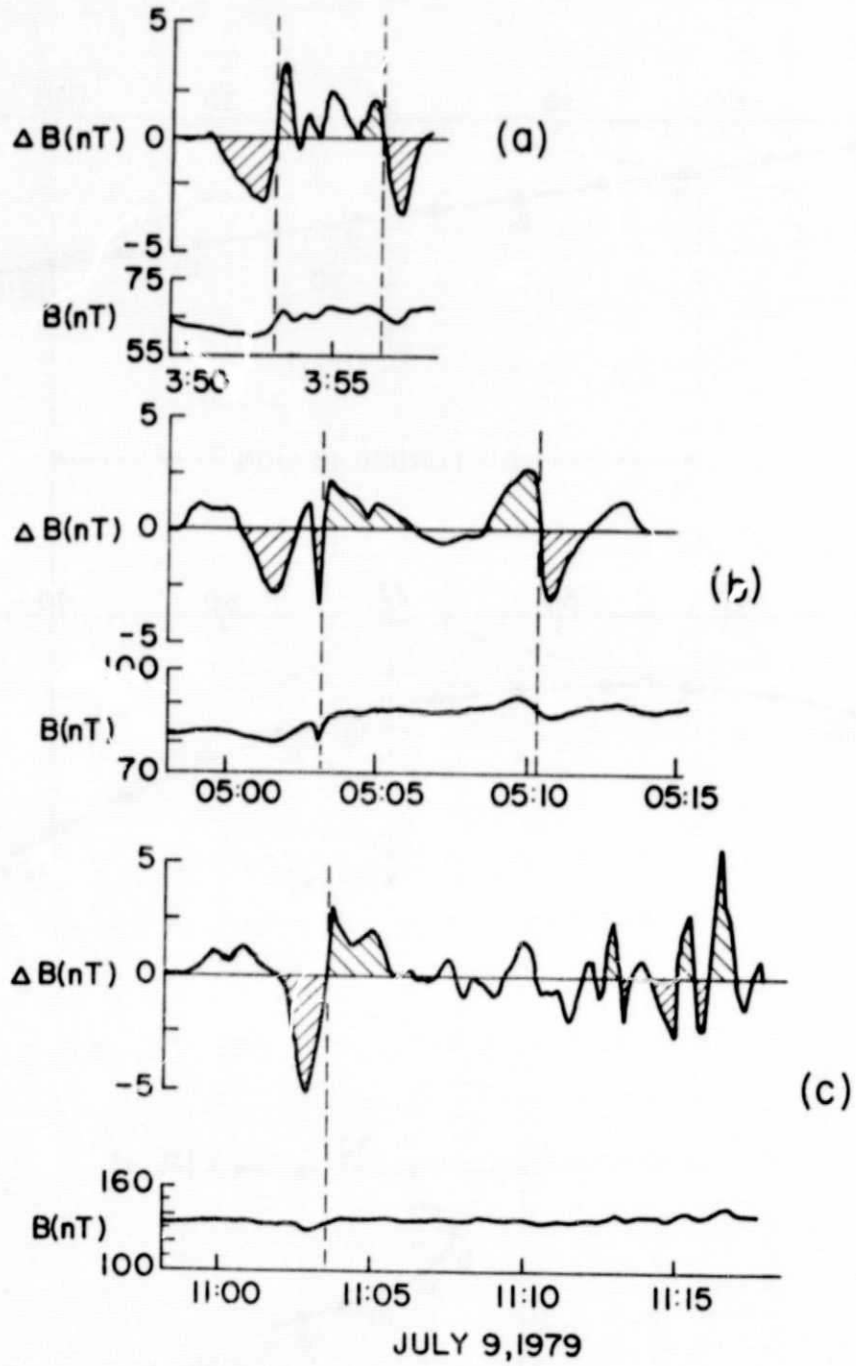


FIGURE 8